Nano World Journal

https://doi.org/10.17756/nwj.2022-098

Research Article

Open Access

An Analysis of Iron Oxide Nanoclusters as Antifungal Agents and *In Silico* Model with Lanosterol 14 α--Demethylase in *Candida albicans*

Heba S. Abbas* **and Tarek A.M. Ismaeil**

Microbiology Department, National Organization for Drug Control and Research (NODCAR), recently, Egyptian Drug Authority, Giza, Egypt

***Correspondence to:**
Heba S. Abbas
Microbiology Department
National Organization for
Drug Control and Research (NODCAR),
Recently, Egyptian Drug Authority, Giza, Egypt
Delegated lecturer, Microbiology Department,
College of Drug and Manufacturing, MISR
University for Science and Technology
Giza, Egypt
E-mail: heba181179@yahoo.com

Received: January 25, 2022
Accepted: April 06, 2022
Published: April 08, 2022

Citation: Abbas HS, Ismaeil TAM. 2022. An Analysis of Iron Oxide Nanoclusters as Antifungal Agents and *In Silico* Model with Lanosterol 14 α--Demethylase in *Candida albicans*. *NanoWorld J* 8(2): 36-41.

Published by United Scientific Group

Abstract

The burden on human health has risen with the infections of *Candida sp.*, and looking for therapy is becoming difficult. Because of its different medical applications, metallic iron oxide NPs attract interest. Therefore, five spherical iron oxide nanoclusters were tested in silico for binding of *Candida sp.* For the purpose of predicting the binding mechanism and energy, each iron oxide nanocluster was docked in the active position of the lanosterol 14 α-demethylase enzyme (CYP51), which is crucial for *Candida sp.* growth. The binding energy range for all test iron oxide nanoclusters was –8.17 to –9.75 Kcal/mol. In general, the molecular docking analysis revealed that increasing the size of the sphere nanoclusters (0.5-1 nm) increases the binding energy within 5TZ. Experimentally, the inhibition zone ranged from 16mm to 13mm. High inhibition zones were received from 50% of *Candida albicans* isolates, and the minimum inhibition concentrations were 256µg/ml for all *Candida albicans* isolates. The current findings suggest that iron oxide nanoclusters can be used as potential antifungal medications.

Keywords

Candida infections, Metallic iron oxide NPs, Lanosterol 14α-demethylase enzyme (CYP51)

Introduction

Fungal infections have become a rising health concern, leading to substantial economic losses in hospitals [1, 2]. About 200 species of Candida exist in the world, but only a few are capable of infecting humans if the immune system is compromised [3]. One of the most common kinds of fungal infections that *Candida* species are responsible for is mucocutaneous candidiasis and invasive candidiasis [4, 5].

A standard treatment for invasive or mucocutaneous candidiasis is the application of antifungal drug classes, such as azoles, polyene, echino-candines and flucytosine. Due to the incorrect use of antifungals, fungi evolved resistant mechanisms against antifungal drugs. Hence, new antifungal alternative methods for better treatment are required [6-8].

Nanoparticles are currently of considerable significance for their biological use, such as metal oxide nanoparticles, as an *antimicrobial* agent. Abo-zeid and Williams have been reported in 2019 for antimicrobial activity of metal oxide NPs [9]. Mainly, metal oxide NPs have been shown to be effective in combating nosocomial bacterial infections in hospitals and overcoming bacterial resistance [10-12]. More recently, abbas et al. (2020 a, b) specifically found the pronounced antifungal efficacy of α- Fe_2O_3 against *C. albicans*, which is due to the excessive production of Reactive Oxygen Species (ROS), and it destroys the cellular con-

stituents and deoxyribonucleic acid damage [13-14].

A docking model study is presented here to understand and investigate the interactions of iron oxide nanoclusters with the lanosterol 14α-demethylase (CYP51) enzyme, which is produced by the (CYP51/ERG11) gene and is necessary to support candida growth. Moreover, the antifungal activity was studied *in vitro* against *Candida albicans*. The heme group of CYP51 proteins in the active site is involved in cytochrome P450, which is a key enzyme in the sterol's production and a vital component of the fungal membrane [15]. The docking model was also applied to determine the potential application of iron oxide nanoclusters in the treatment and controlling candida infections.

Materials and Methodology

Ligand preparation

Using material studio software, the crystal structure of Fe_2O_3 was converted into a three-dimensional form using the American mineralogist's crystal structure database, http://www.minsocam.org/MSA/Crystal_Database.html. We selected five Sphere Fe_2O_3 nanoclusters as a model of Fe_2O_3 to study their inhibitory effect against **CYP51** by molecular docking analysis. This optimized structure was used to construct the sphere nanoclusters using the built-in tools in the material studio program, as follow: Sphere, 0.5 nm (radius = 2.5 Å, Fe = 7, and O=7 atoms), 0.6 nm (radius = 3.0 Å, Fe = 14, and O = 17 atoms), 0.7 nm (radius = 3.5 Å, Fe = 16, and O = 21 atoms), 0.8 nm (radius = 4.0 Å, Fe = 28, and O = 36 atoms), 0.9 nm (radius = 4.5 Å, Fe = 38, and O = 46 atoms), and 1 nm (radius = 5.0 Å, Fe = 42, and O = 56 atoms). The structural optimization of all studied compounds was implemented using the Molecular Mechanics 2 (MM2) force field. After that, using Auto DockTools 1.5.6 software, the structures were transformed to pdbqt format.

Protein preparation

The crystal structure of CYP51 with a potent ligand (VT1161) (PDB code: 5TZ1) was obtained from the Protein Data Bank (www.rcsb.org). The BIOVA Discovery Studio software was used to eliminate small molecules from the crystal structures of 5TZ1 [15].

Molecular docking

The protein was given polar hydrogen and Kollman charges, and a pdbqt format file was created using AutoDock Tools 1.5.6 software. The protein was made with AutoDock Tools 1.5.6's protein preparation wizard. The protein was given polar hydrogen and Kollman charges, and a pdbqt format file was created with AutoDock Tools. 5TZ1 was stripped of all water molecules. The ligands' torsions were determined by first detecting the roots in AutoDock Tools 1.5.6, then setting aromaticity criteria of 7.5. For 5TZ1, we set a grid size of 80Å x80Å x80 Å and used the Lamarckian Genetic Algorithm (LGA) to carry out the molecular docking procedure, as outlined in this paper [16-17].

Size measurement of SIONs

Spherical iron oxide nanoparticles (SIONs) were prepared previously by Dr Heba S Abbas in Microbiology Laboratory (C), Egyptian Drug Authority (previously, National Organization for Drug Control and Research), the size of tested SIONs was characterized by High-Resolution Transmission Electron Microscope (HRTEM).

Antifungal assay of SIONs

The antifungal activity of SIONs was assessed against three clinical strains of C. *albicans*, and *C. albicans* ATCC 10231. The isolates were plated on Sabroud dextrose agar plates for the test. A sterile cork-borer was used to cut the wells into the plates, and 50 µl of SIONs (two-fold serial dilution method (512, 265,128µg/ml)) in DMSO solutions were dispensed in each well. For 24 hours, the plates were kept at 27°C. The inhibitory zone's diameter was measured in millimetres [18]. The minimum inhibitory concentration (MIC) of SIONs was examined [19].

Results and Discussion

Molecular docking

Figure 1 depicts the interactions of all nanoclusters investigated inside 5TZ1. The results of the molecular docking analysis for all Fe_2O_3 sphere nanoclusters examined against 5TZ1 are shown in table 1. The binding energy inside 5TZ1 increased as the size of the sphere nanoclusters grew larger, according to the molecular docking study. So, 1nm Fe_2O_3 nanoclusters exhibited the highest binding energy (-9.17 k.cal/mol) inside 5TZ1, as displayed in Table 1 in the case of 5TZ1. Also, 1nm nanoclusters which revealed the maximum binding energy interact with GLU 473, PHE 463, TYR 353 and LYS 358 amino acid residuals of 5TZ1 through hydrogen bond interaction at distances 2.41, 2.38, 2.32, and 2.18 Å, respectively and with LYS 433, SER 436, and THR 152 through van der walls interactions as shown in figure 1. In case of 0.9 nm Fe_2O_3 nanoclusters, they interact with THR 172, PHE 170, ASP 214 and GLU 174 amino acid residuals of 5TZ1 through hydrogen bond interaction at distances 2.49, 2.42, 2.16, and 2.10 Å, respectively and with SER 175, and ARG 215 through van der walls interactions as shown in figure 1. However, 0.8 nm Fe_2O_3 nanoclusters interact with LEU 87, SER 507, ALA 62 and GLN 65 amino acid residuals of

Table 1: Molecular docking study of Fe2O3 nanoclusters against 5TZ1.

Ligand	Binding Energy (ΔG) k.cal/mol
0.5 nm Fe_2O_3 nanoclusters	-8.17
0.6 nm Fe_2O_3 nanoclusters	-8.36
0.7 nm Fe_2O_3 nanoclusters	-8.68
0.8 nm Fe_2O_3 nanoclusters	-8.87
0.9 nm Fe_2O_3 nanoclusters	-9.22
1 nm Fe_2O_3 nanoclusters	-9.75

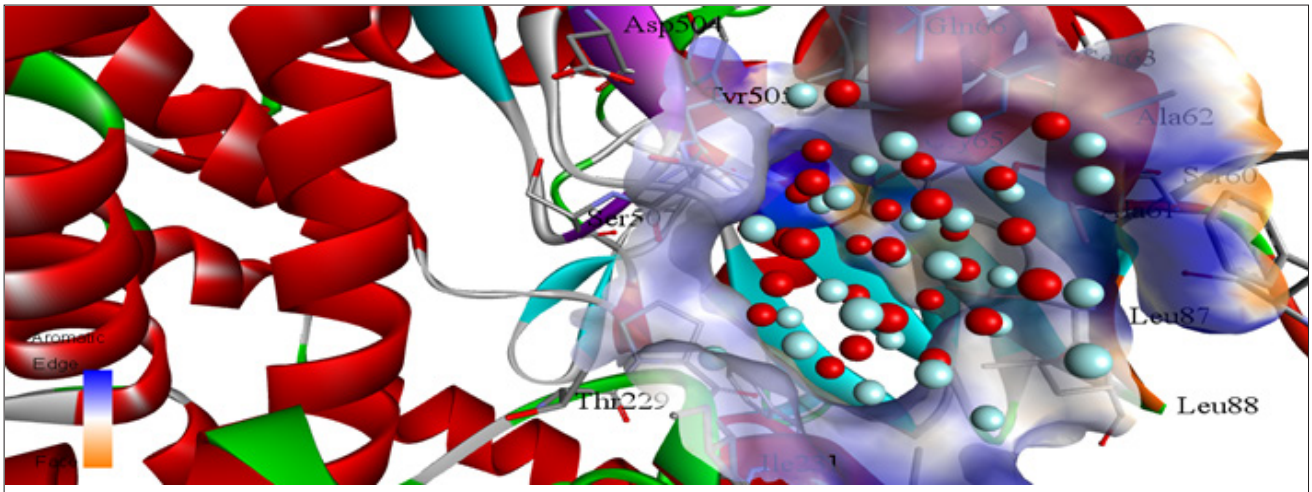

0.8 nm Fe_2O_3 nanoclusters inside 5TZ1 receptor

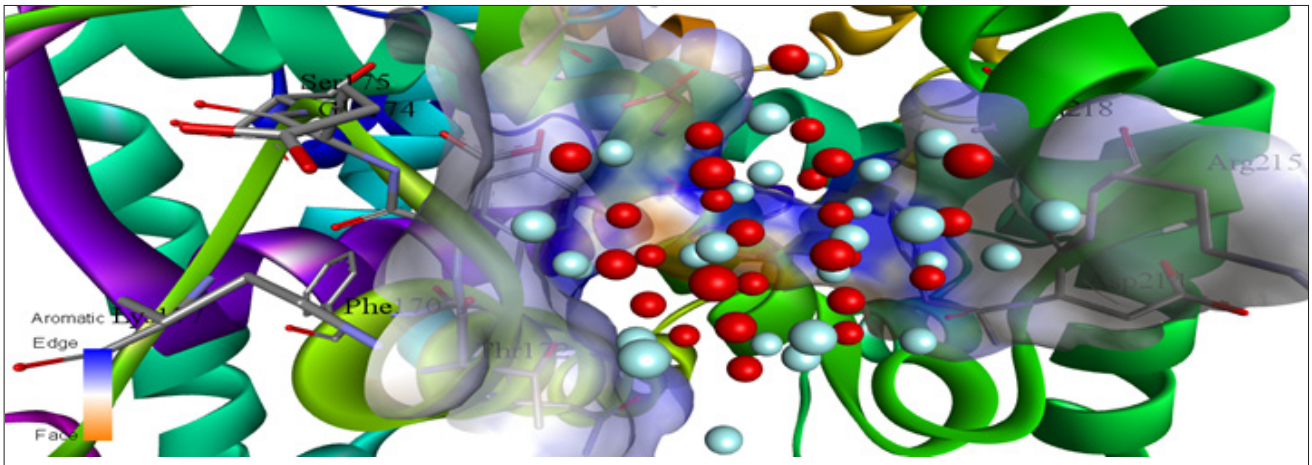

0.9 nm Fe_2O_3 nanoclusters inside 5TZ1 receptor

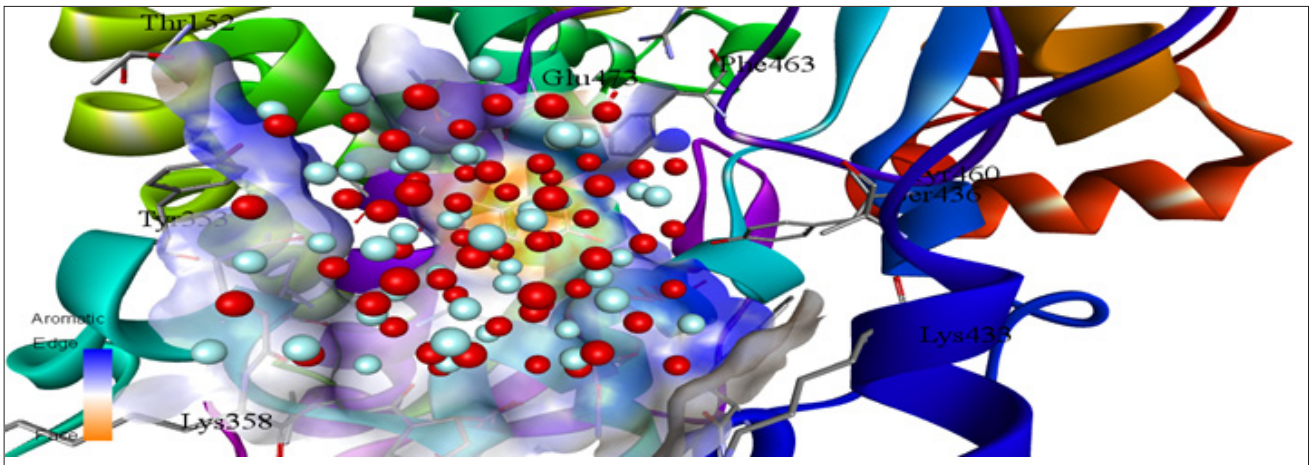

1 nm Fe2O3 nanoclusters inside 5TZ1 receptor

Figure 1: The schematic presentation for the interactions of 0.8- 1 nm Fe2O3 nanoclusters inside 5TZ1 receptor.

5TZ1 through hydrogen bond interaction at distances 2.34, 2.31, 2.33, and 2.11 Å, respectively and with LEU 88, SER 60, and THR 229 through van der walls interactions as shown in figure 1. In addition, 0.7 nm Fe_2O_3 nanoclusters interact with GLN 66, PHE 280, TYR 505 and SER 507 amino acid residuals of 5TZ1 through hydrogen bond interaction at distances 2.47, 2.39, 2.29, and 2.22 Å, respectively and with LEU 87, LYS 90, and ILE 231 through van der walls interactions as shown in figure 2. Also, 0.6 nm Fe_2O_3 nanoclusters interact with SER 506, THR 229, and GLN 66 amino acid residuals

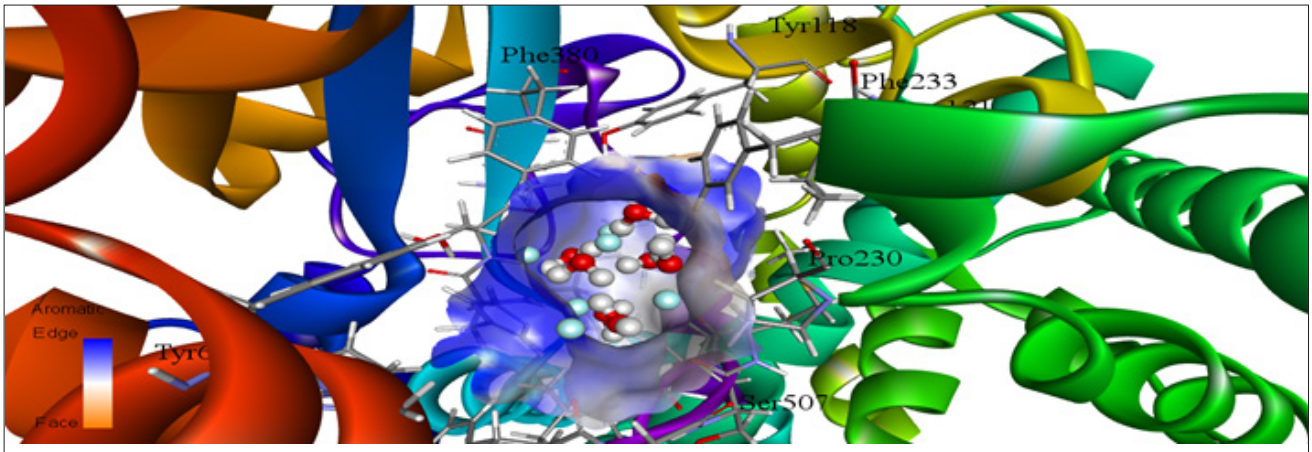

0.5 nm Fe2O3 nanoclusters inside 5TZ1 receptor

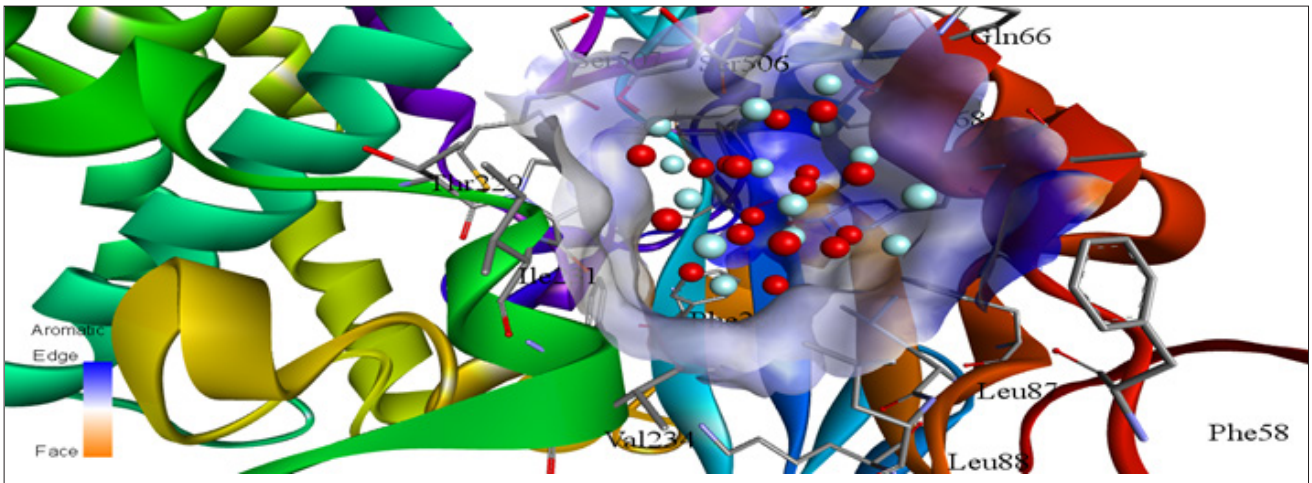

0.6 nm Fe2O3 nanoclusters inside 5TZ1 receptor

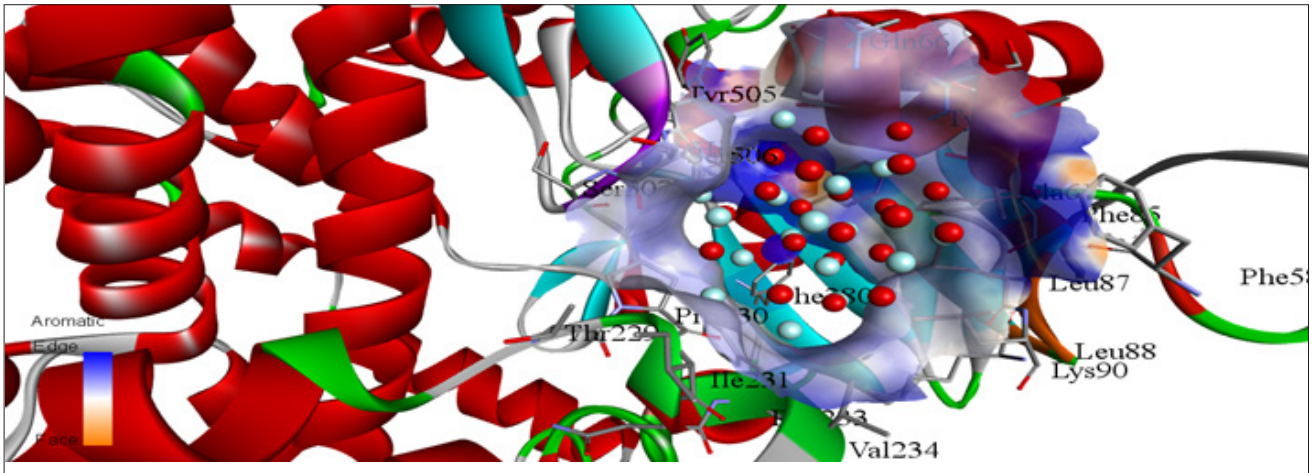

0.7 nm Fe2O3 nanoclusters inside 5TZ1 receptor

Figure 2: The schematic presentation for the interactions of 0.5- 0.7 nm Fe2O3 nanoclusters inside 5TZ1 receptor.

of 5TZ1 through hydrogen bond interaction at distances 2.33, 2.26, and 2.30 Å, respectively and with ILE 231, VAL 234, LEU 88 and PHE 280 through van der walls interactions as shown in Figure 2. Furthermore, 0.5 nm Fe_2O_3 nanoclusters interact with PHE 380, PRO 230, and SER 507 amino acid residuals of 5TZ1 through hydrogen bond interaction at distances 2.45, 2.40and 2.29 Å, respectively and with PHE 233, and TYR 118 through van der walls interactions as shown in figure 2. We can deduce that all studied nanoclusters with different sizes can act as 5TZ1 inhibitors from all the previous discussions. Also, increasing the size of the nanoclusters can lead to an increase in the inhibitory of Fe_2O_3 nanoclusters

against 5TZ1 inhibitors. Finally, a molecular docking study suggested that Fe_2O_3 nanoclusters could be used as inhibitors against CYP51.

HRTEM of SIONs

The shape of iron oxide nanoparticles was found to be spherical with approximately an average diameter of 5.74 ±0.87nm. The diameter was in the range 6.79, 4.62 nm as shown in figure 3.

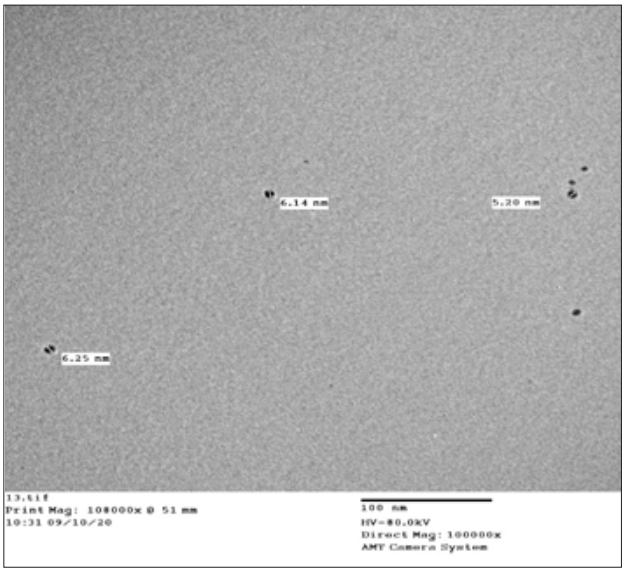

Figure 3: HRTEM image of SIONS.

In vitro evaluation of antifungal activity

The antifungal activity of SIONs has been evaluated using the agar well diffusion method. The SIONs showed antifungal activity compared to negative control (DMSO). The inhibition zone ranged from 16mm to 13mm. High inhibition zones were received from 50% of *Candida albicans* isolates, and the minimum inhibition concentrations were 256µg/ml for all *Candida albicans* isolates (Table 2). Increasing the size of the spherical nanoclusters increased the binding energy within 5TZ1, which is the explanation for SION's antifungal activity, according to the molecular docking study.

According to other research papers, metal oxide NPs, such as ZnO NPs or CuO NPs, have been discovered to exhibit antimicrobial activities compared to iron oxide nanoparticles [20]. However, Abbas et al. 2020 a & b demonstrated the high antibacterial and anti-candidal activities of iron oxide NPs. The following is how the authors explained the ROS production in candida cells by iron oxide nanoparticles: overproduction of reactive oxygen species (ROS) promotes organelle malfunction and apoptosis [12, 13].

Table 2: Antifungal activity of SIONs.

***Candida albicans* strains**	**Diameter of Inhibition Zone (mm)**	**Minimum Inhibitory Concentration (MIC)**
Candida albicans (1)	13	256 µg/ml
Candida albicans (2)	16	256 µg/ml
Candida albicans (3)	16	256 µg/ml
Candida albicans ATCC 10231	14	256 µg/ml
Negative Control	NIL	

Conclusions

Candida infections are a serious health problem. These infections can be superficial, resulting in mucocutaneous candidiasis, or they can spread to the bloodstream and internal organs, resulting in life-threatening invasive illnesses. There are antifungal drugs, but due to the development of fungal resistance, they have drawbacks. As a result, there is a high demand for new antifungal strategies that can control or limit the spread of Candida infections. Herein, a series of spherical iron oxide nanoclusters was tested in silico. The binding mechanism and binding energy of the test iron oxide nanoclusters could be anticipated in each case by docking them in the active site of fungal CYP51.The docking results show that for each iron oxide nanoclusters, the binding mode of each test interacts with at least four amino acid residues in the active site of fungal CYP51. We found that increasing the size of the sphere nanoclusters improved the binding energy. Also, in vitro antifungal activity of 5.74 ± 0.87nm of the sphere iron oxide nanoparticles were assessed. The minimum inhibitory concentrations were 256µg/ml against *C. albicans*. In the future, we recommend iron oxide nanoclusters to proceed with in vivo study for the treatment of Candida infections.

Funding Information

No Fund was provided for this article.

Ethical Approval

There is no Ethical approval needed for this article.

Acknowledgement

None.

Conflict of Interest

None.

References

1. Cuenca-Estrella M, Bernal-Martínez L, Buitrago MJ, Castelli MV, Gomez-Lopez A, et al. 2008. Update on the epidemiology and diagnosis of invasive fungal infection. *Int J Antimicrob Agents* 32(Suppl 2): 143-147. https://doi.org/10.1016/S0924-8579(08)70016-5
2. Olaechea PM, Palomar M, León-Gil C, Álvarez-Lerma F, Jordá R, et al. 2004. Study group economic impact of *candida* colonization and *candida* infection in the critically ill patient. *Eur J Clin Microbiol Infect Dis* 23(4): 323-330. https://doi.org/10.1007/s10096-004-1104-x
3. Spampinato C, Leonardi D.: 2013. Candida infections, causes, targets, and resistance mechanisms: traditional and alternative antifungal agents. *Biomed Res Int* 2013: 204237. https://doi.org/10.1155/2013/204237

4. Desai JV, van de Veerdonk FL, Lionakis MS. 2017. Understanding the role of host immune responses in invasive candidiasis. *Intensive Care Med* 44(8): 1310-1314. https://doi.org/10.1007/s00134-017-4988-5
5. Kullberg BJ, Arendrup MC. 2015. Invasive Candidiasis. *N Engl J Med* 373: 1445-1456. https://doi.org/10.1056/NEJMra1315399
6. Rezaei Z, Khabnadideh S, Zomorodian K, Pakshir K, Kashi G, et al. 2011. Design, synthesis and antifungal activity of some new imidazole and triazole derivatives. *Arch Pharm (Weinheim)* 344(10): 658-665. https://doi.org/10.1002/ardp.201000357
7. Gonçalves SS, Souza ACR, Chowdhary A, Meis JF, Colombo AL. 2016. Epidemiology and molecular mechanisms of antifungal resistance in Candida and Aspergillus. *Mycoses* 59(4): 198-219. https://doi.org/10.1111/myc.12469
8. Masiá-Canuto M, Gutiérrez-Rodero F. 2002. Antifungal drug resistance to azoles and polyenes. *Lancet Infect Dis* 2(9): 550-563. https://doi.org/10.1016/S1473-3099(02)00371-7
9. Abo-zeid Y, Williams GR. 2019. The potential anti-infective applications of metal oxide nanoparticles: A systematic review. *Wiley Interdiscip Rev Nanomed Nanobiotechnol* 12(2): e1592. https://doi.org/10.1002/wnan.1592
10. Imai K, Ogawa H, Bui VN, Inoue H, Fukuda J, et al. 2012. Inactivation of high and low pathogenic avian influenza virus H5 subtypes by copper ions incorporated in zeolite-textile materials. *Antiviral Res* 93(2): 225-233. https://doi.org/10.1016/j.antiviral.2011.11.017
11. Nahhal IM, Elmanama AA, Amara NM. 2016. Synthesis of nanometal oxide–coated cotton. Intech. https://doi.org/10.5772/63505
12. Abbas HS, Krishnan A, Katakonta M. 2020a. Antifungal and antiovarian cancer properties of α Fe2O3 and α Fe2O3 /ZnO nanostructures synthesized by *Spirulina platensis*. *IET Nanobiotechnol* 14(9): 774-784. https://doi.org/10.1049/iet-nbt.2020.0055
13. Abbas HS, Krishnan A, Katakonta M. 2020b. Fabrication of iron oxide/zinc oxide nanocomposite using creeper *blepharis maderaspatensis* extract and their antimicrobial activity. *Front Bioeng Biotechnol* 8: 595161. https://doi.org/10.3389/fbioe.2020.595161
14. Abbas HS, Krishnan A. 2020. Magnetic nanosystem to combat pathogenic fungi. *Adv Pharm Bull* 10(4): 512-523. https://doi.org/10.34172/apb.2020.063
15. Rabelo VW, Santos TF, Terra L, Santana MV, Castro HC, et al. 2017. Targeting CYP51 for drug design by the contributions of molecular modeling. *Fundam Clin Pharmacol* 31(1): 37-53. https://doi.org/10.1111/fcp.12230
16. Dassault systèmes BIOVIA, Discovery studio modeling environment. 2017. San Diego: Dassaul Systèmes.
17. Trott O, Olson AJ. 2010. AutoDock Vina: improving the speed and accuracy of docking with a new scoring function, efficient optimization, and multithreading. *J Comput Chem* 31(2): 455-461. https://doi.org/10.1002/jcc.21334
18. Thomas R, Jasim B, Mathew J, Radhakrishnan EK. 2012. Extracellular synthesis of silver nanoparticles by endophytic Bordetella sp. isolated from *Piper nigrum* and its antibacterial activity analysis. *Nano Biomed Eng* 4(4): 183-187. https://doi.org/10.5101/nbe.v4i4.p183-187
19. Shanmugaiah V, Harikrishnan H, Al-Harbi NS, Shine K, Khaled JM, et al. 2015. Facile synthesis of silver nanoparticles using Streptomyces sp. VSMGT1014 and their antimicrobial efficiency. *Dig J Nanomater Biostruct* 10(1): 179-187.
20. Horst AK. 2009. Antimicrobial effects of metal oxide nanoparticles. pp. 12-13.